

## Electrooptic Characteristics of the Fringe-Field Switching Device with Electrode on Top Substrate

Hyang Yul KIM, Seung Ho HONG, Tae Kyu PARK, Dae-Shik SEO<sup>1</sup>, John Moon RHEE<sup>2</sup> and Seung Hee LEE<sup>2\*</sup>

Cell Process Development Group, Hyundai Display Technology, San 136-1, Ami-ri, Bubal-eup, Ichon-si, Kyungki-do 467-701, Korea

<sup>1</sup>Department of Electrical and Computer Engineering, Yonsei University, Seoul 12-749, Korea

<sup>2</sup>Department of Polymer Science and Technology, Chonbuk National University, Chonju, Chonbuk 561-756, Korea

(Received April 9, 2001; accepted for publication September 5, 2001)

The homogeneously aligned nematic liquid-crystal (LC) display driven by the fringe-field is known to exhibit high light efficiency as well as a wide viewing angle unlike the conventional in-plane switching (IPS) mode, with pixel and common electrodes existing only on the bottom substrate. We found that when a common electrode exists on the top and bottom substrates, the device with some advantages in fabrication and quality still reveals high transmission and a wide viewing angle with LC having a negative dielectric anisotropy. In this paper, the switching mechanism and electro-optic characteristics of the device with the electrode on the top substrate are investigated. [DOI: 10.1143/JJAP.41.176]

KEYWORDS: liquid-crystal display, fringe-field switching, in-plane switching, electro-optic characteristics

### 1. Introduction

A liquid crystal display (LCD) associated with the transition from homogeneous alignment to in-plane rotation using the fringe field has been reported previously.<sup>1–3)</sup> The device is named a fringe field switching (FFS) device, and is known to exhibit a wide viewing angle and high light transmission simultaneously unlike the in-plane switching (IPS) device.<sup>4,5)</sup> Studies on electro-optic characteristics of the FFS device, such as their dependence on the rubbing direction,<sup>6)</sup> sign of the dielectric anisotropy, and shape of the pixel electrode<sup>7,8)</sup> have been carried out previously. In a conventional FFS device, the pixel and counter electrodes exist only on the bottom substrate with some distance between the pixel electrodes so that with bias voltage, a fringe field that has both horizontal and vertical field components is generated, whereas only the horizontal field is generated in the IPS device. The fringe field rotates the LC molecules almost in plane above the entire electrode surface when LCs with negative dielectric anisotropy are used, giving rise to high transmittance and a wide viewing angle.

In this paper, we propose a new device that also has the counter electrode on the top substrate. This changes the field distribution when the voltage is applied. Therefore, an understanding of the LC dynamics corresponding to the field and electro-optic characteristics of the new device is important because the device has advantages in terms of the easy fabrication of LCD and the reduction of residual image.<sup>9)</sup> We found that deformation of the LC corresponding to the applied voltage depends on the dielectric anisotropy of the LC, that is, the LC with negative dielectric anisotropy is much more advantageous in light efficiency than that with positive dielectric anisotropy, and the new device needs a slightly higher voltage and higher retardation value for maximum transmission than those in the conventional device. In this paper, the switching mechanism and electrooptic characteristics of the new device in comparison with those of the conventional one have been investigated by simulation and experiment.

### 2. Field Distribution and Profile of the LC Director in the FFS Device

Figure 1 shows cell structures of the conventional and the new FFS devices where the LCs are in homogeneous alignment with the optical axis, which coincides with one of the crossed polarizers at an initial state. In the conventional FFS device, the pixel and common electrodes exist only on the bottom substrate. However, in the new device, the electrode on the top substrate is connected to the common electrode on the bottom substrate and thus the field distribution along the horizontal and vertical axes is quite different from that in the conventional one, as shown by the equipotential lines. In both FFS devices, the pixel and common electrodes are transparent conductors like indium-tin-oxides (ITOs).

In the device with uniaxial LC medium under the crossed polarizers, the conventionalized light transmission is given by

$$T/T_0 = \sin^2(2\psi) \sin^2(\pi d \Delta n / \lambda),$$

where  $\psi$  is the angle between the crossed polarizers and the LC director,  $\Delta n$  is the birefringence of the liquid crystal medium,  $\lambda$  is the wavelength of an incident light and  $d$  the cell gap. Therefore, the FFS device appears to be black in the absence of a field and, in the presence of a field, the LC director starts to deviate from the optical axis of the crossed polarizers, giving rise to light transmission. When  $\psi$  is  $45^\circ$  on average, the transmission becomes maximum.

The cell conditions for simulations and experiments in this work are the same as those reported in the previous work.<sup>6)</sup> The LCs with negative dielectric anisotropy are aligned to be  $12^\circ$  from the horizontal component of the fringe field at the initial state and the thickness of the ITO on the top substrate is  $1300 \text{ \AA}$ . The simulation program of 2 dimMos from autronic-Melchers is used to simulate the device and the elastic constants of the LC,  $K_{11}$  (splay),  $K_{22}$  (twist) and  $K_{33}$  (bend) are 13.5 pN, 6 pN and 15.1 pN, respectively.

To clarify the electrooptic characteristics of the new device, it is necessary to clarify the profile of the LC director corresponding to the field. First, we calculated the field distribution along the horizontal axis at several vertical distances. Figures 2 and 3 show the distribution of the field

\*To whom correspondence should be addressed. E-mail address: lsh1@moak.chonbuk.ac.kr

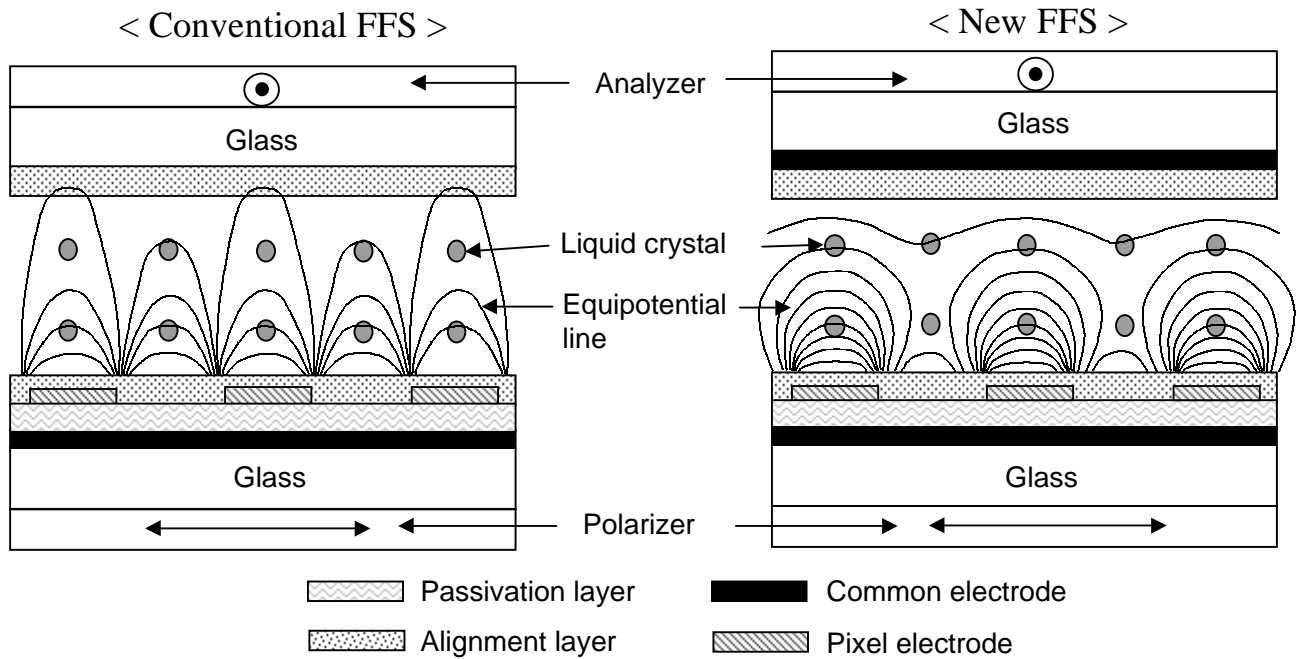


Fig. 1. Cell structures of the conventional and new FFS devices with ITO on top substrate.

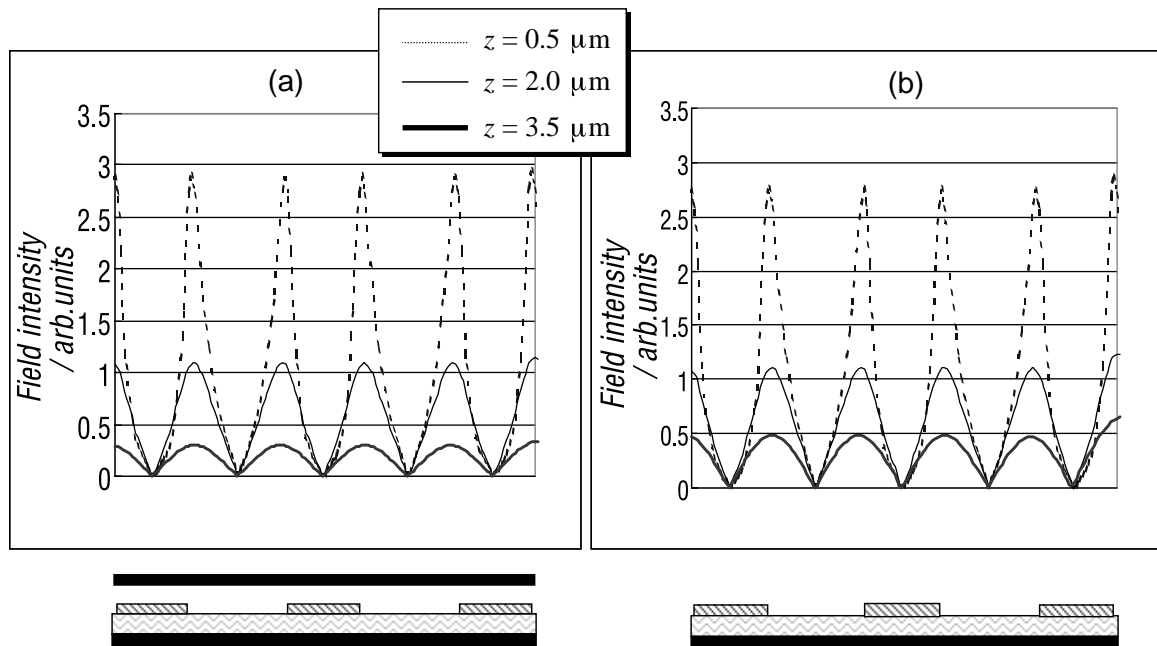


Fig. 2. Field distribution of the horizontal component in (a) new and (b) conventional FFS devices along the horizontal axis at several vertical distances.

intensity of the vertical ( $E_z$ ) and horizontal ( $E_y$ ) components along the horizontal direction in the conventional and new FFS devices when a voltage of 5 V is applied. As indicated, the distribution form of  $E_y$  along the horizontal axis is about the same for both devices, that is, the field intensity of  $E_y$  around the edge of the pixel electrodes is maximal and rapidly drops to zero above the center of the electrodes. The field intensity also decreases rapidly away from the electrode surface. This implies that the deformation of the LC is much stronger near the bottom surface than near the top surface. The maximum horizontal field intensity around the electrode

edges is about the same for both devices. However, it is weaker in the new device than those in the conventional device at  $z = 3.5 \mu\text{m}$ . In the case of  $E_z$ , the maximum field intensity exists near the region between the edge and the center of the electrodes, although it is much weaker than that of  $E_y$ . Furthermore, the vertical field intensity in the new FFS device is much stronger above the center of the pixel electrodes at all vertical distances and weaker above the center of the common electrodes than that in the conventional device near the bottom surface. Such a difference in the field distribution drives the LCs to deform in different

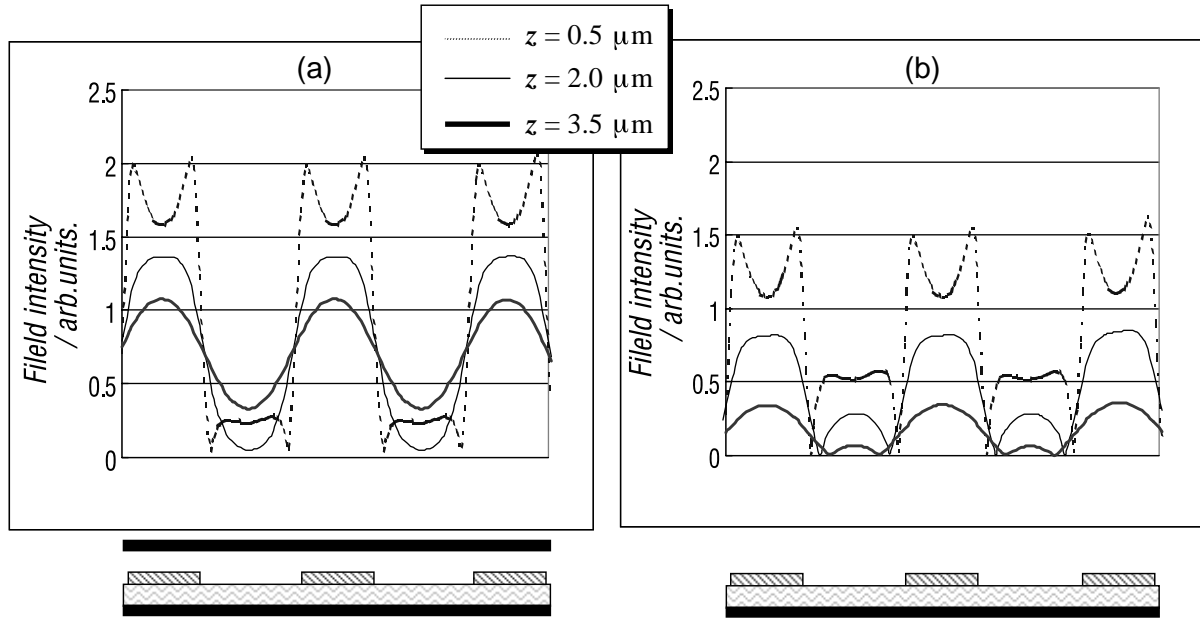


Fig. 3. Field distribution of the vertical component in (a) new and (b) conventional FFS devices along the horizontal axis at several vertical distances.

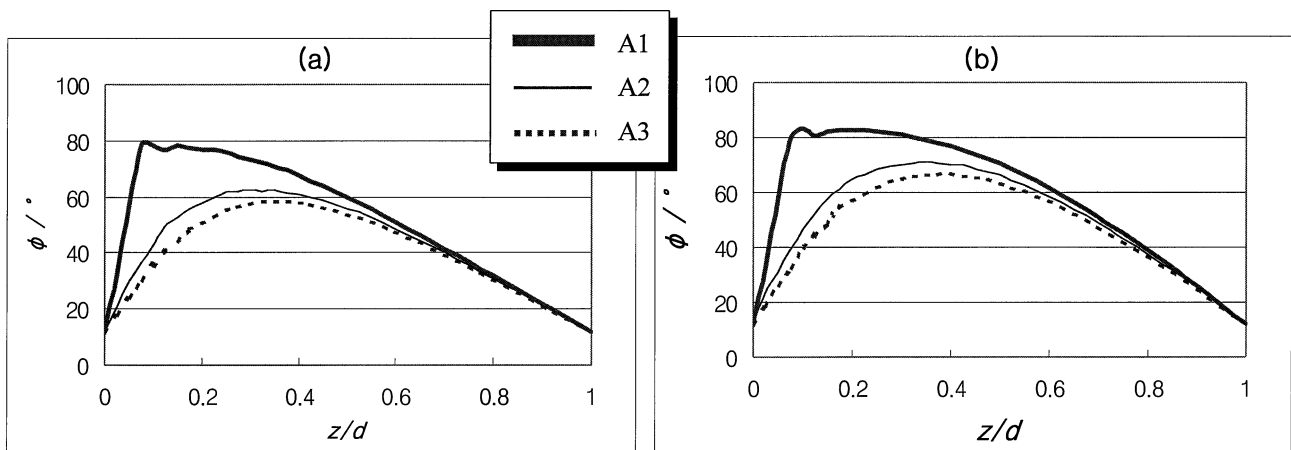


Fig. 4. Profile of the LC director in twist angle along the LC layers in (a) new and (b) conventional FFS devices.

ways in both devices. Figure 4 shows the profile of the LC molecules in twist angle ( $\Phi$ ) along the LC layers at three positions, that is, at the edge (A1), between the edge and the center (A2) and above the center (A3) of the pixel electrodes. When a voltage of 5 V is applied, the maximum degree of the twist angle of the LC molecules at positions A1, A2, and A3 is slightly smaller in the new device than that in the conventional device. It is twisted less than  $48^\circ$  from the initial twist angle of  $12^\circ$  for the new device while it is larger than  $48^\circ$  for the conventional device at position A3. This indicates that the existence of the electrode on the top substrate increases the field intensity of  $E_z$ , hindering the twist deformation of the LC molecules above the pixel electrodes. Figure 5 shows the profile of the LC molecules in tilt angle ( $\theta$ ) along the LC layers at three different positions. At A1, the maximum tilt angle for the conventional device is  $-8^\circ$  while it is  $-12^\circ$  (where the negative sign means the tilt angle opposite to the initially defined tilt angle) for the new device. In addition, the  $\theta$  is higher for the new device than

for the conventional one, in almost all LC layers along the vertical direction at positions A1 and A2.

### 3. Electro-optic Characteristics of the New Device

For electrooptic measurement, the LCD-7000 (Otsuka Electronics, Japan) is used. The halogen lamp was used as a light source and a square wave, 60 Hz voltage source from the function generator was applied to the sample cell. The light passing through the cell was detected by a photomultiplier tube.

Figure 6 shows the measured voltage-dependent transmittance ( $V$ - $T$ ) curves in the conventional and new FFS devices. The results show that the  $V$ - $T$  curve of the new device slightly shifts to the right, and consequently the operational voltage at which the transmission becomes maximal increases, although the threshold voltage at which the light transmission starts is about the same. These results can be well understood from the field distribution of the new device. With the common electrode on the top substrate, the

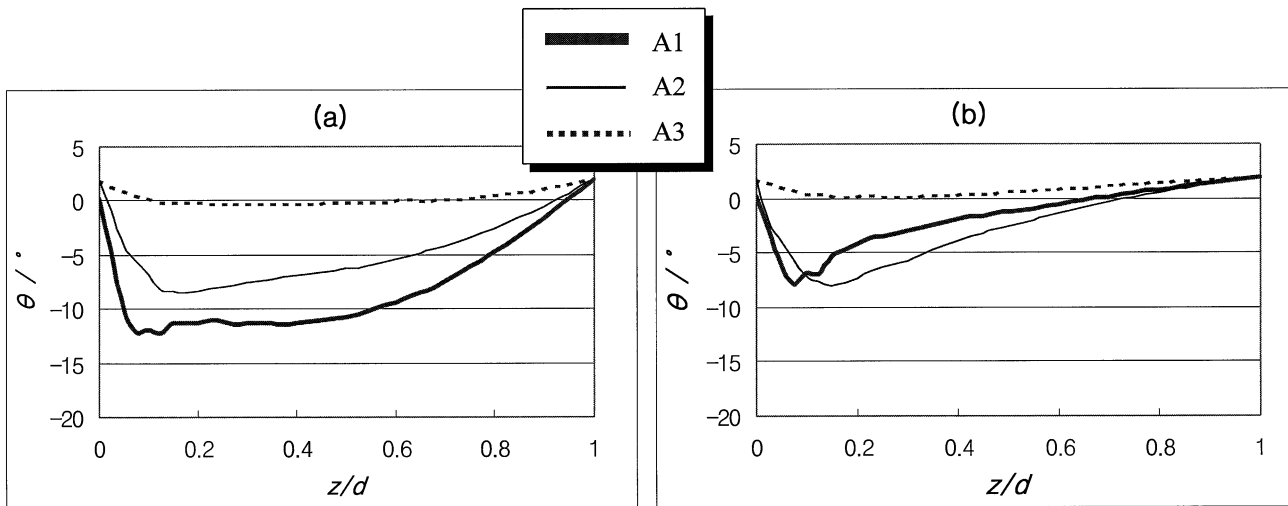


Fig. 5. Profile of the LC director in tilt angle along the LC layers in (a) new and (b) conventional FFS devices.

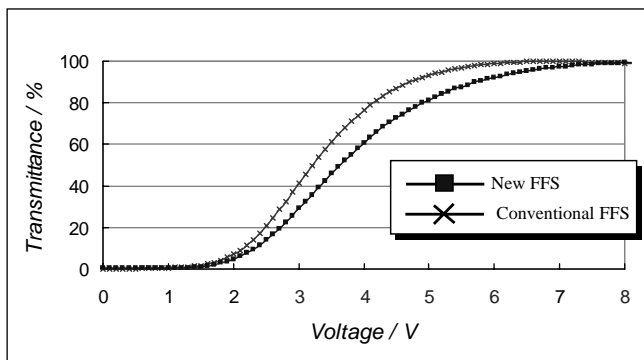


Fig. 6. Voltage-dependent transmittance curves in conventional and new FFS devices.

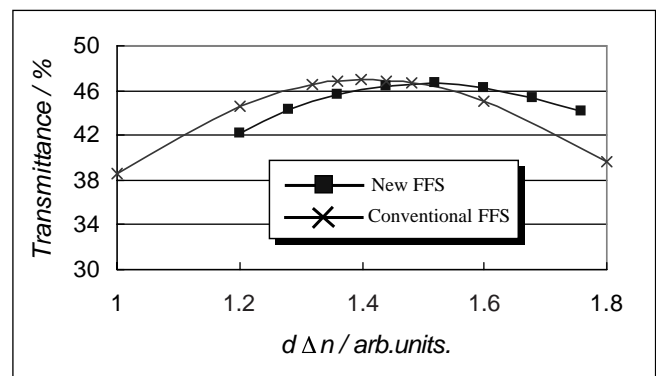


Fig. 8. Transmission as a function of retardation of the FFS cell.

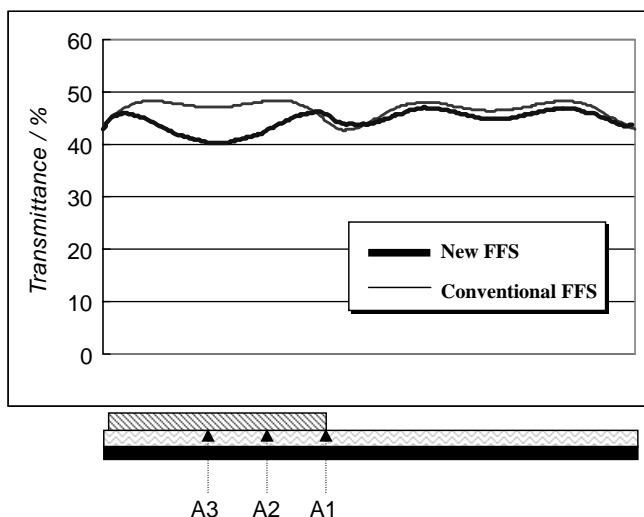


Fig. 7. Calculated light transmission along horizontal axis for both devices.

intensity of the vertical field above the pixel electrode becomes stronger than that of the device without the electrode and thus the tilt angle of the LC molecules is larger for the new device than that for the conventional one,

thus reducing the twist angle slightly in the new device. The smaller twist angle means a smaller transmittance, explaining the lower light transmission for the new device than that for the conventional one at the applied voltage. Figure 7 shows the calculated light transmission along the horizontal axis at an applied voltage of 5 V. The transmission above the pixel electrode in the new device is lower than that in the conventional device, clearly explaining the low transmission of the new device due to the low twist angle at a given voltage. Furthermore, the increase in tilt angle of the LC molecules changes the optimal retardation value of the cell for maximum transmission. As indicated in the equation for transmission, the effective retardation value for maximum light efficiency is about  $\lambda/2$  and can be changed by the tilt up of the LC molecules when a voltage is applied. That is, for a higher tilt angle of the LC molecules, the device needs a higher retardation value of the LC cell for maximum light efficiency. We have calculated the light transmission as a function of the retardation value, as indicated in Fig. 8. For the calculated data, the light transmission from surfaces with horizontal range of  $69 \mu\text{m}$  that includes 8 pixel electrodes was counted. In this case the voltage in which gives the maximum light transmission was applied. The result shows that the new device needs higher retardation value than the conventional one. We have investigated the viewing angle characteristics. In the off-state, both devices show exactly

the same characteristics in terms of the leakage of light since the molecular alignment is the same. In the on-state, the profile of the LC director is slightly different from that in the off-state as mentioned and thus both devices show slightly different results. Figures 9(a) and 9(b) show measured iso-luminance contours for both devices in the on-state with applied voltage of 6.4 V, where 90%, 75%, 50% and 25% indicate the light intensities relative to that in the normal direction. Comparing both results in detail, the decreased rate of the light intensity from the conventional direction is slightly less for the conventional device than for the new device, that is, the area of each iso-luminance line having an ellipse shape is large in the conventional device. Furthermore, we have examined the difference between the maximum and the minimum light transmittances along all azimuthal directions for given polar angles from normal to 70°, as indicated in Fig. 9(c). A smaller difference in value indicates a better uniformity of light transmission as the viewing angle is varied. Up to 40° of the polar angle, the difference is about the same but it is smaller for the conventional device than that for the new device, indicating slightly large viewing angle dependence with the new

device. Nevertheless, in consideration of the contrast ratio, both devices show almost the same results since the light leakage in the off-state is the same. We have also measured the response time for both devices. The falling time associated with restoring force of the LC director to the initial state after releasing the voltage to zero is 26 ms, which is the same for both devices. However, the rising times associated with molecular dynamics responding to the applied voltage are not the same for both devices. They are 33 ms and 26 ms for the new and the conventional devices, respectively. The reason that rising response time becomes larger in the new device is due to the twist deformation with the generation of a higher tilt angle in the new device than in the conventional device.

We have also calculated the light efficiency of the new FFS device using the LCs with positive dielectric anisotropy. In the positive LCs, the LC orients parallel to an electric field. That is, the LCs above the pixel electrode tilt up much higher than negative LCs instead of twisting due to strong vertical field intensity above that region. Therefore, the device gives rise to a very low light efficiency, about 40% of that with negative LCs for the same retardation.

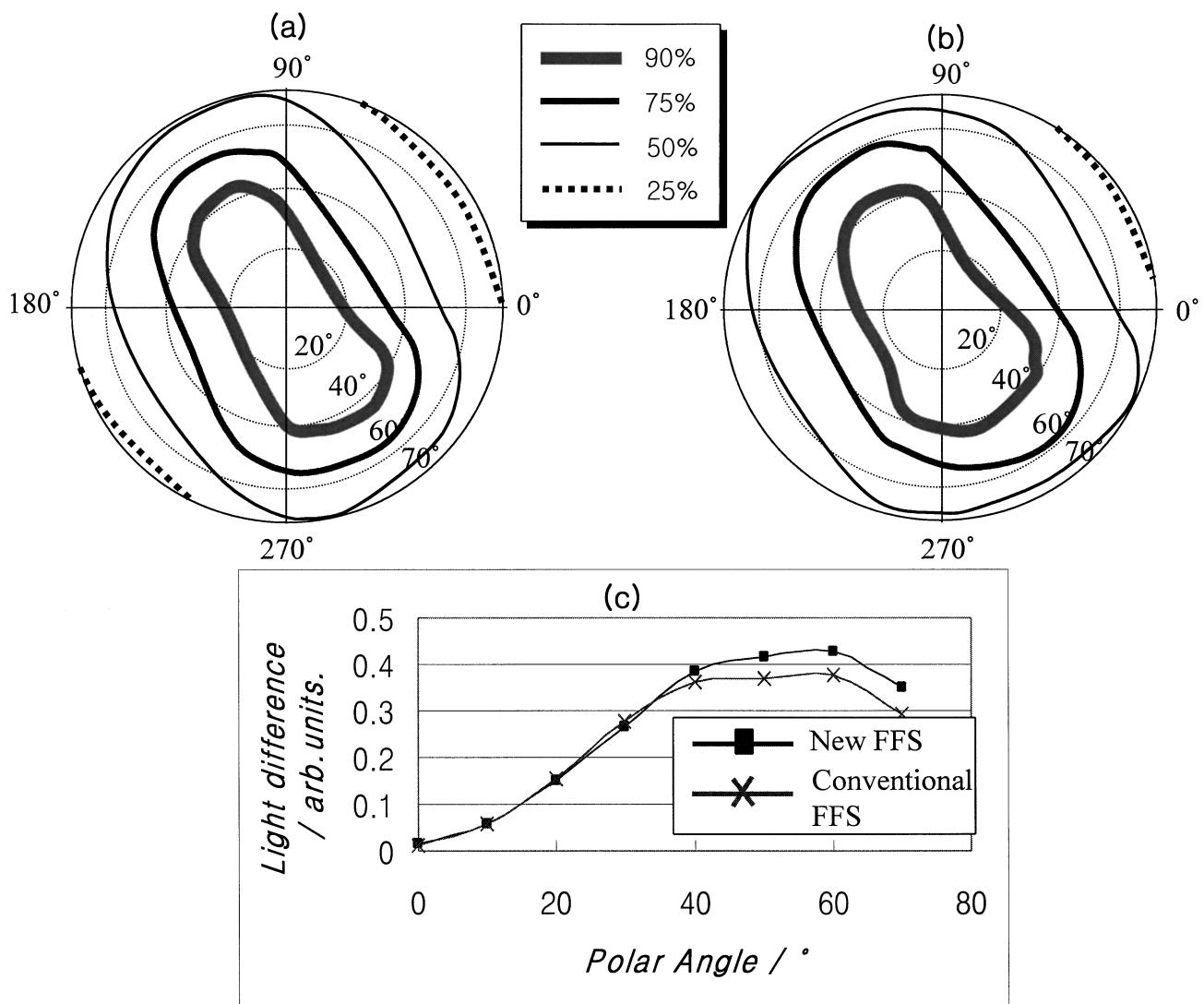


Fig. 9. Iso-luminance contours of conventional (a) and new (b) FFS devices at an applied voltage of 6 V and (c) the difference between minimal and maximal transmittances along all directions with increasing polar angle.

#### 4. Summary

We have proposed a new FFS device that has a counter electrode on both the top and bottom substrates, and the electro-optic characteristics of the new FFS device have been studied by experiments and simulation. In the new device, the driving voltage is slightly increased, the cell needs a higher retardation for maximal light efficiency in the new device than in the conventional device, the LCs with negative dielectric anisotropy are very effective in terms of light efficiency, and the viewing angle characteristic is only slightly decreased. The results are important for the design of a new device with ease of manufacturing and reduction of the residual image of the FFS-LCD.

1) S. H. Lee, S. L. Lee and H. Y. Kim: Proc. 18th Int. Display Research

Conf., Seoul, 1998, p. 371.

- 2) S. H. Lee, S. L. Lee and H. Y. Kim: Appl. Phys. Lett. **73** (1998) 2881.
- 3) S. H. Lee, S. L. Lee, H. Y. Kim and T. Y. Eom: Dig. Tech. Pap. 1999 Society for Information Display Int. Symp., San Jose, 1999, p. 202.
- 4) M. Oh-e, M. Ohta, S. Aratani and K. Kondo: Proc. 15th Int. Display Research Conf., Hamamatsu, 1995, p. 577.
- 5) K. Kondo, S. Matsuyama, N. Konishi and H. Kawakami: Dig. Tech. Pap. 1998 Society for Information Display Int. Symp., Anaheim, 1998, p. 389.
- 6) S. H. Hong, I. C. Park, H. Y. Kim and S. H. Lee: Jpn. J. Appl. Phys. **39** (2000) L527.
- 7) S. H. Lee, S. L. Lee, H. Y. Kim and T. Y. Eom: J. Kor. Phys. Soc. **35** (1999) S1111.
- 8) S. H. Lee, S. M. Lee, H. Y. Kim, J. M. Kim, S. H. Hong, Y. H. Jeong, C. H. Park, Y. J. Choi, J. Y. Lee, J. W. Koh and H. S. Park: Dig. Tech. Pap. 2001 Society for Information Display Int. Symp., San Jose, 2001, p. 484.
- 9) H. Y. Kim and S. H. Lee: private communication.